



Phenolics profile and antioxidant activities of *in vitro* propagules and field-raised plant organs of *Curculigo latifolia*

Abdul Halim Umar¹ , Diah Ratnadewi^{2*} , Mohamad Rafi³ , Yohana Caecilia Sulistyaningsih² ,
Hamim Hamim² 

¹Division of Pharmaceutical Biology, College of Pharmaceutical Sciences Makassar, STIFA Makassar, Makassar, Indonesia.

²Department of Biology, Faculty of Mathematics and Natural Sciences, IPB University, Bogor, Indonesia.

³Department of Chemistry, Faculty of Mathematics and Natural Sciences, IPB University, Bogor, Indonesia.

ARTICLE INFO

Received on: 08/11/2022
Accepted on: 12/02/2023
Available Online: 28/03/2023

Key words:

Callus, chemometrics,
Hypoxidaceae, metabolomics,
secondary metabolite,
UHPLC-Q-Orbitrap HRMS.

ABSTRACT

Curculigo latifolia is traditionally used in herbal medication. We determined the total phenolics profile, antioxidant capacity, and metabolomics of *in vitro* propagules compared to the mother plant organs, intending to disclose the prospective of *in vitro* cultured propagules as an alternative source of the essential metabolites of this species. Phenolic content was investigated by colorimetry. Antioxidant activities were determined by 1,1-diphenyl-2-picrylhydrazyl (DPPH), 2,2'-azino-bis(3-ethylbenzothiazoline-6-sulfonic acid) (ABTS), and ferric reducing/antioxidant power (FRAP) assays. Ultrahigh-performance liquid chromatography-quadrupole-orbital ion trap analyzer-high-resolution mass spectrometry (UHPLC-Q-Orbitrap HRMS) and chemometrics were exploited for comparative analyses of the metabolite's composition. Total phenolic contents varied from 152.19 to 457.80 gallic acid equivalent g⁻¹. The lowest DPPH and ABTS radical scavenging activities with the IC₅₀ values were obtained from the rhizome, and FRAP-reducing power activities were found in the leaves. UHPLC-Q-Orbitrap HRMS data and multivariate analysis classified and differentiated the compounds in the callus, plantlet leaves, rhizomes, petioles, and leaves. The marker compounds discriminating the *in vitro* propagules from the mother plant organs are orcinol glucoside, nyasicoside, and vanillin. This information would be valuable for the pharmaceutical industry, herbalists, or herbal medicine producers in using the plant organs as well as the *in vitro* callus.

INTRODUCTION

Curculigo latifolia (family: Hypoxidaceae), locally known as "Marasi," is an annual plant commonly found in Southeast Asia, including Indonesia. Some tribes in Indonesia, the Batak Karo (Sumatra), use this species as an ornamental garden plant, traditional healthcare, and food additive (Silalahi and Nisyawati, 2018). Recent studies have shown that *C. latifolia* has high phenolic content and significantly exhibits antioxidant and α -glucosidase inhibitor activities (Umar *et al.*, 2021a). The

main components that had pharmacological activities included 1,1-bis-(3,4-dihydroxyphenyl)-1-(2-furan)-methane, (1S,2R)-*O*-methylnyasicoside, 2,4-dichloro-5-methoxy-3-methylphenol, curculigoside B and curculigosaponin G, H, and I, orchioside B, and orcinol glucoside (Umar *et al.*, 2021a). The other groups of compounds identified in *Curculigo* spp. were phenolic glucoside, norlignans, and terpenoids (Wang *et al.*, 2021), with various bioactivities, such as anti-inflammatory (Zhu *et al.*, 2015a), neuroprotection (Zhao *et al.*, 2020), antidepressant (Zhang *et al.*, 2017), antiosteoporosis and anti-rheumatoid arthritis (Han *et al.*, 2020), and sweet-tasting and taste-modifying (Okubo *et al.*, 2021). Callus extract of *C. latifolia* also has antioxidant and antibacterial effects (Farzinebrahimi *et al.*, 2016).

The culture technology of cell/callus, tissue, and plant organs has proven to be an efficient method for producing secondary metabolites from a plant (Li *et al.*, 2021). The metabolites can be

*Corresponding Author

Diah Ratnadewi, Department of Biology, Faculty of Mathematics and Natural Sciences, IPB University, Bogor, Indonesia.

E-mail: dratnadewi@apps.ipb.ac.id

produced in a sustainable system without environmental constraints due to biotic and abiotic conditions. Temperature, light exposure, nutrient availability, and pH can be easily controlled under *in vitro* system (Cabañas-García *et al.*, 2021). Therefore, *in vitro* culture is a potential tool to obtain compounds with selected biological activities, particularly from uncultivated plants like *C. latifolia* in Indonesia.

Compounds in *in vitro* propagules can be identified quickly using a metabolomic approach (Kim *et al.*, 2021). This approach provides an overview of all the metabolites present in plant tissues. Complex metabolomic data need to be supported by chemometric techniques, that is, principal component analysis (PCA) and partial least squares (PLS), to help discriminate, group, and identify the essential compounds as well as the marker metabolites of the analyzed samples (Bertol *et al.*, 2021). Phenolic content, antioxidant activity, and phenolics profiling in callus, plantlet leaves, and organs of *C. latifolia* have never been investigated. The phenolics profile of the *in vitro* propagules and the mother plant organs in this study was determined by ultrahigh-performance liquid chromatography-quadrupole-orbital ion trap analyzer-high-resolution mass spectrometry (UHPLC-Q-Orbitrap HRMS). It helped group samples based on similarities and differences in compounds and identified any marker metabolites distinguishing the two types of samples. It is necessary to distinguish the essential metabolites in the mother plant organs and *in vitro* propagules, mainly when the latter are to be developed as an alternative plant source (Kim *et al.*, 2021). We give more profound knowledge of the phytochemicals contained in the *in vitro* propagules and in the mother plant organs of this species, along with their potential as antioxidants.

MATERIAL AND METHODS

Chemicals and reagents

Gallic acid, 1,1-diphenyl-2-picrylhydrazyl (DPPH), 1,3,5-tri(2-pyridyl)-2,4,6-triazine, and 6-hydroxy-2,5,7,8-te-

tramethyl-chroman-2-carboxylic acid (Trolox) were purchased from Sigma Aldrich (St Louis). Water [liquid chromatography-mass spectrometry (LC-MS grade)], acetonitrile (LC-MS grade), methanol (LC-MS grade), formic acid, aluminum chloride, Folin Ciocalteu reagent, sodium carbonate, ferric chloride, ethanol, and sodium tetraborate were from Merck (Darmstadt, Germany).

Plant material

The plant materials of *C. latifolia* were obtained from Puncak District, Sinjai Regency (South Sulawesi), Indonesia (5°13'25"S, 120°02'46"E, ± 959 m.asl), in February 2019 (rainy season). The samples were identified based on the published flora and voucher specimens deposited at the Herbarium Bogoriense, Research Center for Biology, the Indonesian Institute of Sciences, Indonesia, under voucher number 184. The plants collected from the field were planted in pots under greenhouse conditions in Bogor (West Java), from which explants for callus culture were taken. The media for callus initiation, proliferation, and regeneration were MS (Murashige and Skoog, 1962) with 3 mg^l⁻¹ 6-benzylaminopurine (BAP) and 5 mg^l⁻¹ indole-3-butyric acid (IBA). The detailed tissue culture method for callus initiation and plantlet regeneration has been described in Umar *et al.* (2021b). The callus and plantlet leaves (Fig. 1) were then used for this study.

Sample preparation

The samples from the callus of *C. latifolia* (CCL), plantlet leaf of *C. latifolia* (PLL), and from the rhizome, petiole, and leaf of *C. latifolia* originating from Sinjai-Puncak Sinjai-Puncak (RLSK, PLSK, and LLSK, respectively) were prepared as previously described by Umar *et al.* (2021a). Sinjai-Puncak is situated in South Sulawesi.

Determination of total phenolics

Total phenolic content (TPC) was determined using the method described by Umar *et al.* (2021a). Phenolic content

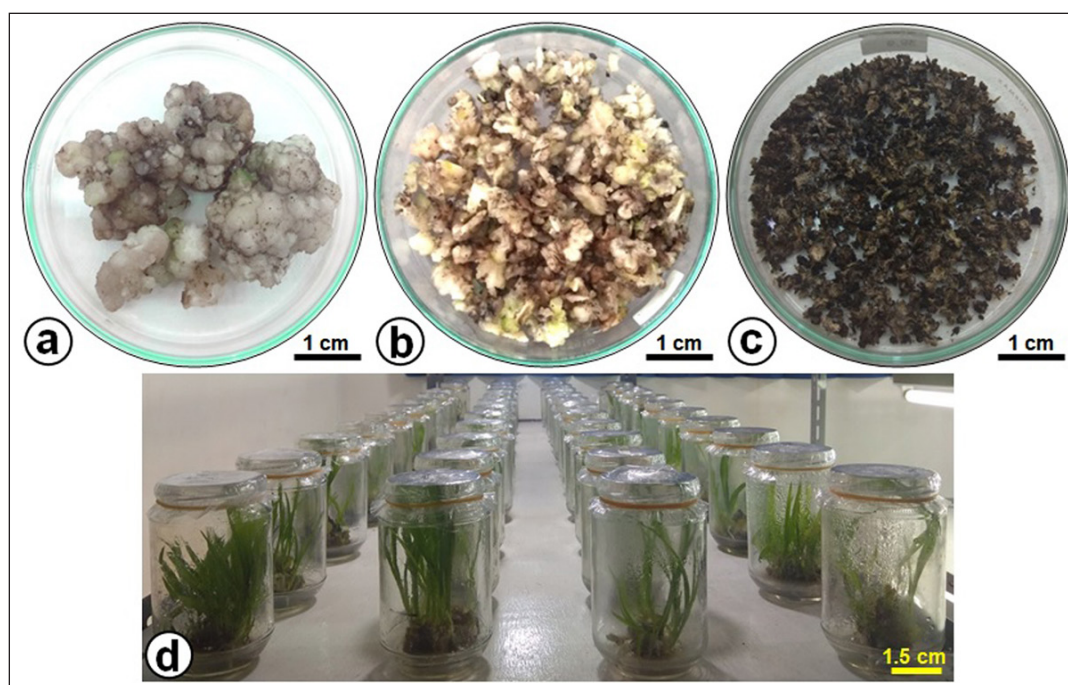


Figure 1. The yield of *in vitro* culture of *C. latifolia*. (a) Freshly harvested callus, (b) chopped callus, (c) dried callus used for extraction, and (d) plantlets grown on MS culture medium with a BAP-IBA combination.

was expressed as gallic acid equivalent (mg GAE g⁻¹). For each sample, this assay was replicated three times.

Determination of antioxidant activities

DPPH free radical scavenging activity

The DPPH free radical scavenging activity of sample extracts was measured in 96-well plates, according to the procedure described in Umar *et al.* (2021a) with slight modifications. An aliquot of 10 µl of appropriately diluted sample or Trolox solution (31.25–1000 µM) was added to 190 µl of DPPH solution (in ethanol). The mixture was incubated at 37°C for 30 minutes, and the absorbance was measured at 517 nm. All samples and the control were tested in triplicate. The ability to scavenge the DPPH radical was calculated as a percentage as follows:

$$\text{DPPH (scavenging effect)\%} = [(A_{\text{DPPH}} - A_s) / A_{\text{DPPH}}] \times 100,$$

where A_{DPPH} is the absorbance of the control, and A_s is the absorbance of the sample. The IC₅₀ value was determined to be the effective concentration at which DPPH radicals were inhibited by 50%. In addition, to determine the IC₅₀ of samples on DPPH, a series of six different concentrations were used. The ethanol instead of the sample was made as a blank control, while Trolox was used as the standard.

2,2'-azino-bis(3-ethylbenzothiazoline-6-sulfonic acid) (ABTS) free radical scavenging activity

We used the procedure of Zhu *et al.* (2015b) to determine the antioxidant activity by the ABTS assay. About 10 µl of the sample was diluted appropriately. Then, 190 µl of ABTS⁺ solution was added to a 96-well plate. This assay was replicated three times. Trolox was used as the standard. The equation used to determine the antioxidant activity followed the DPPH scavenging method described above. The scavenging activities of different concentrations of samples against ABTS⁺ would also result in the IC₅₀.

Ferric reducing/antioxidant power (FRAP) assay

As described previously by Zhu *et al.* (2015b), a FRAP assay was performed in this study. Approximately 10 µl of properly diluted samples and 30 µl of distilled water were added to 260 µl of freshly prepared FRAP reagent in a 96-well plate. The mixture was incubated at 37°C for 10 minutes. The absorbance of the reaction mixture was measured at 593 nm by a microplate reader. It was carried out in triplicate. The calibration curve was plotted on a FeSO₄·7H₂O standard at a concentrations range of 0.125 to 2 mM, and FRAP activity was expressed as mmol Fe²⁺ equivalent per g sample (mmol Fe²⁺ equivalent g⁻¹). A high FRAP value indicates a greater antioxidant capacity.

UHPLC-Q-Orbitrap HRMS analysis

The extraction and analysis procedure followed exactly the method described by Umar *et al.* (2021a). Metabolite profiling was performed in an Orbitrap High-Resolution Mass Spectrometer (Vanquish Flex UHPLC-Q Exactive Plus) using Accucore™ Phenyl Hexyl (100 × 2.1 mm, 2.6 µm) as the separation column and UV detector at 254 nm (Thermo Scientific™, Waltham, MA). Rhizome, petiole, and leaves collected from the field were dried for 3 days in a drying cabinet at 40°C. About 250 mg of fresh

callus and plantlet leaves were dried and extracted in the same way. All samples were analyzed in three replications.

Data analysis

Data of total phenolics and the determination of antioxidant activity (DPPH, ABTS, and FRAP) were expressed as means ± SD of three replicates for each sample. The data were statistically analyzed using R ver. I386 3.6.0 (R Core Team, 2018). Data from UHPLC-Q-Orbitrap HRMS analysis were proceeded to the Compound Discoverer™ Software (Thermo Scientific™, Waltham, MA), MS-DIAL ver. 4.70, and MS-FINDER ver. 3.52 (Tsugawa *et al.*, 2015). The compounds identification used an in-house database and MSP File (in MS/MS positive and negative mode). Clustering analysis was performed using PCA and hierarchical clustering analysis (HCA). A supervised PLS discrimination analysis (PLS-DA) helped to evaluate the differences in metabolite levels. An orthogonal partial least square discriminant analysis (OPLS-DA) assisted in identifying the marker compounds in *in vitro* propagules (CCL and PLL) and mother plant organs (RLSK, PLSK, and PLSK). The results were subjected to several validation tools such as R² and Q² (permutation value) and variables of importance in projection (VIP) to confirm the reliability of the PLS-DA and OPLS-DA model. Finally, analysis of variances was performed to determine significant differences, if any, with a 95% confidence level by MetaboAnalyst 5.0 (<https://www.metaboanalyst.ca>) (Chong *et al.*, 2019).

RESULTS

TPC

The TPC of the dried extracts of callus, plantlet leaves, rhizomes, leaves, and petiole is listed in Table 1. The rhizome's TPC was the highest (457.80 ± 0.51 mg GAE g⁻¹), followed by plantlet leaves, callus, petiole, and leaves.

Antioxidant activity

In this work, we used three different methods, DPPH, ABTS, and FRAP assays, to assess and compare the antioxidant potential of *in vitro* propagules and plant organs. The results are shown in Table 1. Antioxidant activity of the rhizome was significantly the highest, followed by plantlet leaves, callus, petiole, and leaves, reflected by the DPPH and ABTS radical scavenging activities. The antioxidant activities corroborated with the TPC in the tissues. The antioxidant activity increased as the TPC increased in each organ. However, FRAP gave the highest value to leaves.

Metabolites in *in vitro* propagules and plant organs

Representative chromatogram from UHPLC-Q-Orbitrap HRMS for callus (CCL), plantlet leaf (PLL), and rhizome organ (RLSK), petiole (PLSK), and leaf (LLSK) of *C. latifolia* with MS full scan type (100–1,500), relative abundance (0–100), and retention time (0–32 minutes) showed differences in peaks, height, and peak area at the retention times of 1.3–3.7, 4.5–8.5, 9.0–11, 12.0–18.0, and 22.0–26.0 (Fig. S1).

The heatmap analysis with the sample group model (Fig. 2) represents the phenolic compounds identified in each sample group. In general, the distribution of compounds identified in

Table 1. Total phenolics content and antioxidant activity of *in vitro* propagules and plant organs of *C. latifolia*.

Samples	TPC	DPPH	ABTS	FRAP
	(mg GAE g ⁻¹)	IC ₅₀ (mg ml ⁻¹)	IC ₅₀ (mg ml ⁻¹)	(mmol Fe ²⁺ g ⁻¹)
Callus	346.58 ± 1.78 ^c	62.93 ± 0.93 ^d	73.18 ± 0.59 ^c	437.16 ± 0.59 ^c
Plantlet leaves	398.53 ± 0.63 ^d	51.09 ± 2.05 ^c	56.89 ± 1.74 ^{bc}	388.67 ± 1.01 ^b
Rhizome	457.80 ± 0.51 ^e	45.74 ± 0.58 ^b	49.90 ± 1.54 ^b	304.73 ± 3.00 ^a
Leaves	152.19 ± 1.46 ^a	447.03 ± 0.20 ^f	502.74 ± 1.55 ^e	995.39 ± 1.94 ^e
Petiole	300.69 ± 1.97 ^b	212.56 ± 1.04 ^e	224.18 ± 3.64 ^d	782.73 ± 6.70 ^d
Trolox	nt	0.11 ± 0.05 ^a	0.12 ± 0.01 ^a	nt

mmol as mmol Fe²⁺/g of sample, nt: not tested.

Mean values with different lowercase letters within a row were significantly different at $p < 0.05$ by Welch's test.

in vitro propagules (callus and plantlet leaves) was in positive (Fig. 2a) and negative (Fig. 2b) modes, and they were more abundant (on the right-hand side) than those in the mother plant organ samples.

The phenolic compounds identified in the samples are shown in Table 2, in [M + H]⁺ and [M - H]⁻ modes, but the majority were in negative than positive mode. Phenolic groups dominated the compounds in all samples. Alkaloids, saponins, steroids, and terpenoids were also found. All tentative compounds are summarized in Table S1, including the retention time, type of adduction, molecular formula, experimental m/z, MS and MS/MS fragments, accuracy (ppm), and classes of metabolites.

Multivariate analysis

Multivariate statistical analysis was used to classify the differences between callus, plantlet leaves, and mother plant organs (rhizome, petiole, and leaves) of *C. latifolia*, and the results are presented in the PCA (Fig. 3a and b) and HCA (Fig. 3c and d). Unsupervised PCA revealed that the total PC value of the two main components was 100% (PC-1 94.1% and PC-2 5.9%) (Fig. 3a). The HCA showed four clusters, that is, a, b, c, and d (Fig. 3c). Cluster c demonstrated the similarity between callus, leaves, rhizome, and petiole. In the negative mode (Fig. 3b), the total PC value of the two main components was 99.1% (PC-1 92.3% and PC-2 6.8%). The cluster analysis also resulted in four clusters (Fig. 3d). Samples belonging to the same cluster indicated the presence of similar compounds. HCA was made using a dendrogram model with Euclidean distance parameters, a complete clustering algorithm, and auto scale standardization between groups, with 3.0e+08 and 1e+08 similarity for positive and negative modes, respectively.

A supervised PLS-DA was applied to see the patterns of discrimination using a score plot (Fig. S2a and b) and the essential features (Fig. 4a and b). The score plots in positive and negative modes revealed total component values of 99.9% and 99.1%, respectively. In contrast, metabolites with VIP values > 1 were orcinol glucoside in positive mode, and nyasicoside and orcinol glucoside were in negative mode.

The OPLS-DA loadings S-plot (the essential features) (Fig. 5a and b) demonstrated that orcinol glucoside and vanillin were the marker compounds, separating the *in vitro* propagules (IVP = CCL and PLL) and the mother plant organs (OPO = RLSK, LLSK, and PLSK) in the positive mode and nyasicoside

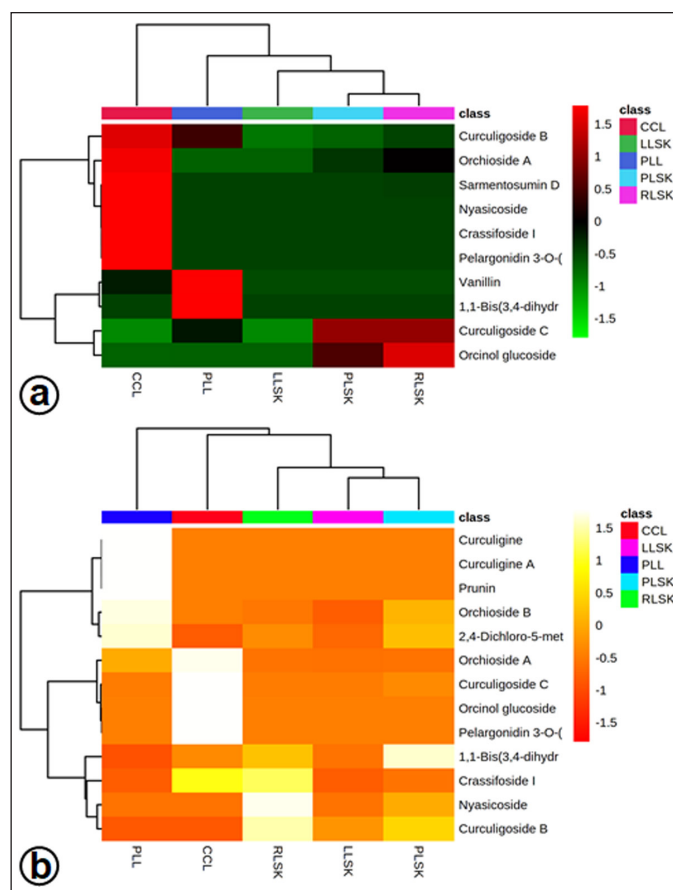


Figure 2. Heatmap analysis representing phenolic compounds identified in callus (CCL), plantlet leaf (PLL), rhizome (RLSK), petiole (PLSK), and leaf (LLSK) organ of *C. latifolia*. The color scale shows the relative abundance of each compound. Each row represents a compound, and each column represents a sample group. (a) Positive and (b) negative mode.

and orcinol glucoside in the negative mode. The OPLS-DA score plot produced a total T score of 72.6% in positive mode and 59.1% in negative mode (Fig. S3a and b). The OPLS-DA model showed a good level of goodness-of-fit ($R^2 = 0.814$) and had a high predictability level ($Q^2 = 0.693$) in positive mode and $R^2 = 0.864$ and $Q^2 = 0.781$ in negative mode (Fig. S4a and b).

Table 2. Phenolic compounds identified in 70% ethanol extract of callus, plantlet leaves, rhizome, leaf, and petiole of *C. latifolia* in positive [M + H]⁺ and negative [M – H][–] modes.

No.	Retention time [min]	Adduction	Formula	Tentative identification	Fragments MS and MS/MS	Part	Chemical type
[M+H] ⁺							
1	0.92	[M+H] ⁺	C ₁₇ H ₁₄ O ₅	1,1-bis(3,4-dihydroxyphenyl)-1-(2-furan)-methane	166.072	PL	Phenolic
2	1.33	[M+H] ⁺	C ₈ H ₈ O ₃	Vanillin	150.981; 137.018; 136.015; 129.113	CC, PL, RL, LL	Phenolic
3	2.33	[M+H] ⁺	C ₂₃ H ₂₄ O ₁₁	Crassifoside I	457.114; 445.114; 387.108	CC, RL	Phenolic
4	7.49	[M+H] ⁺	C ₂₃ H ₂₆ O ₁₁	Nyasicoside	479.152	CC, RL	Phenolic
5	14.02	[M+H] ⁺	C ₂₄ H ₂₃ O ₁₃	Pelargonidin 3- <i>O</i> -(6- <i>O</i> -malonyl-beta- <i>D</i> -glucoside)	433.113; 271.061	CC, RL, LL	Flavonoid
6	14.81	[M+H] ⁺	C ₂₁ H ₂₄ O ₁₁	Curculigoside B	290.271; 276.244	CC, PL, RL, LL, PE	Phenolic glycosides
7	15.07	[M+H] ⁺	C ₂₂ H ₂₆ O ₁₁	Orchioside A	350.143; 213.143	CC, PL, RL, LL	Phenolic glycosides
8	15.44	[M+H] ⁺	C ₃₀ H ₄₂ O ₉	Sarmentosumin D	769.279; 759.295; 691.232	CC	Flavanone
9	21.24	[M+H] ⁺	C ₁₃ H ₁₈ O ₇	Orcinol glucoside	269.100; 256.121; 254.993; 251.093; 237.020	PL, RL	Phenolic glycosides
10	24.02	[M+H] ⁺	C ₂₂ H ₂₆ O ₁₂	Curculigoside C	465.139; 421.112	PL, RL	Phenolic glycosides
[M–H] [–]							
1	0.90	[M–H] [–]	C ₁₇ H ₁₄ O ₅	1,1-bis(3,4-dihydroxyphenyl)-1-(2-furan)-methane	281.045; 269.081	CC, PL, RL, LL, PE	Phenolic
2	3.29	[M–H] [–]	C ₁₃ H ₁₈ O ₇	Orcinol glucoside	285.105	CC, PL, RL, PE	Phenolic glycosides
3	5.83	[M–H] [–]	C ₂₃ H ₂₈ O ₁₂	Curculigine	315.148; 161.109	RL	Chlorophenols glucosides
4	13.62	[M–H] [–]	C ₂₄ H ₂₃ O ₁₃	Pelargonidin 3- <i>O</i> -(6- <i>O</i> -malonyl-beta- <i>D</i> -glucoside)	285.170; 257.175; 243.159	CC	Flavonoid
5	14.57	[M–H] [–]	C ₂₂ H ₂₆ O ₁₁	Orchioside A	449.108; 447.129; 435.129	CC, PL, RL, LL, PE	Phenolic glycosides
6	15.54	[M–H] [–]	C ₂₃ H ₂₆ O ₁₀	Orchioside B	443.134; 433.150; 371.113	CC, PL, LL, PE	Phenolic glycosides
7	15.97	[M–H] [–]	C ₂₃ H ₂₄ O ₁₁	Crassifoside I	457.114; 445.114; 387.108	CC, LL	Phenolic
8	17.59	[M–H] [–]	C ₂₂ H ₂₆ O ₁₂	Curculigoside C	463.124; 453.140; 451.124	CC, PL	Phenolic glycosides
9	20.65	[M–H] [–]	C ₂₀ H ₂₈ Cl ₂ O ₁₂	Curculigine A	529.099	PL, LL	Phenolic glycosides
10	22.10	[M–H] [–]	C ₂₃ H ₂₆ O ₁₁	Nyasicoside	459.129; 449.145; 447.129	CC, PL, RL, LL	Phenolic
11	23.49	[M–H] [–]	C ₂₁ H ₂₂ O ₁₀	Prunin	273.076; 179.034	PL	Flavanone glycoside
12	24.12	[M–H] [–]	C ₂₁ H ₂₄ O ₁₁	Curculigoside B	433.114; 423.129	PL, RL, LL	Phenolic glycosides
13	31.20	[M–H] [–]	C ₈ H ₈ Cl ₂ O ₂	2,4-dichloro-5-methoxy-3-methylphenol	176.987; 174.972; 154.990; 150.972	PL, RL, LL, PE	Phenolic

CC: callus (CCL), PL: plantlet leaves (PLL), RL: rhizome (RLSK), LL: leaf (LLSK), PE: petiole (PLSK).

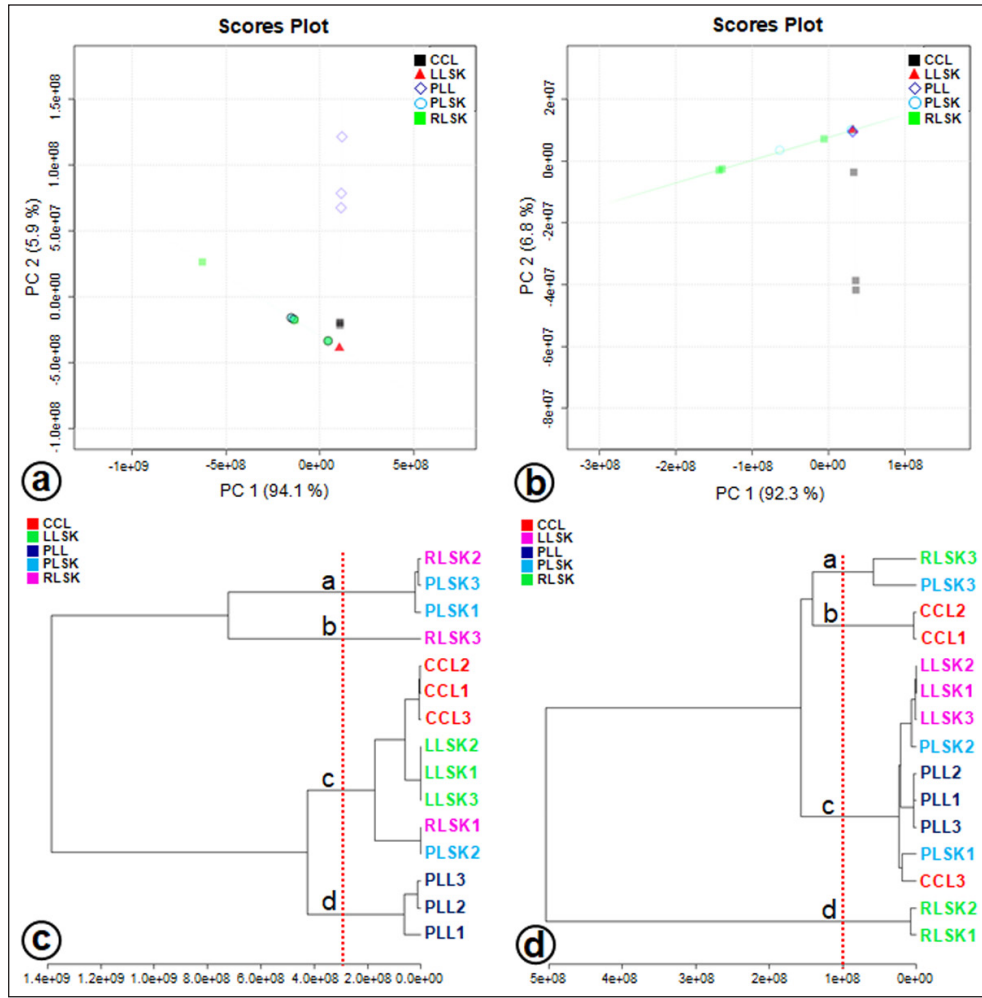


Figure 3. Factorial distribution of principal components 1 (PC1) and 2 (PC2) in (a) positive and (b) negative modes generated from UHPLC-Q-Orbitrap-HRMS data of ethanol extracts of *in vitro* propagules and mother plant organs and hierarchical cluster analysis (HCA) plot, showing four clusters at positive mode (c) and negative mode (d) (n = 3 replicates). Colors indicate the types of samples.

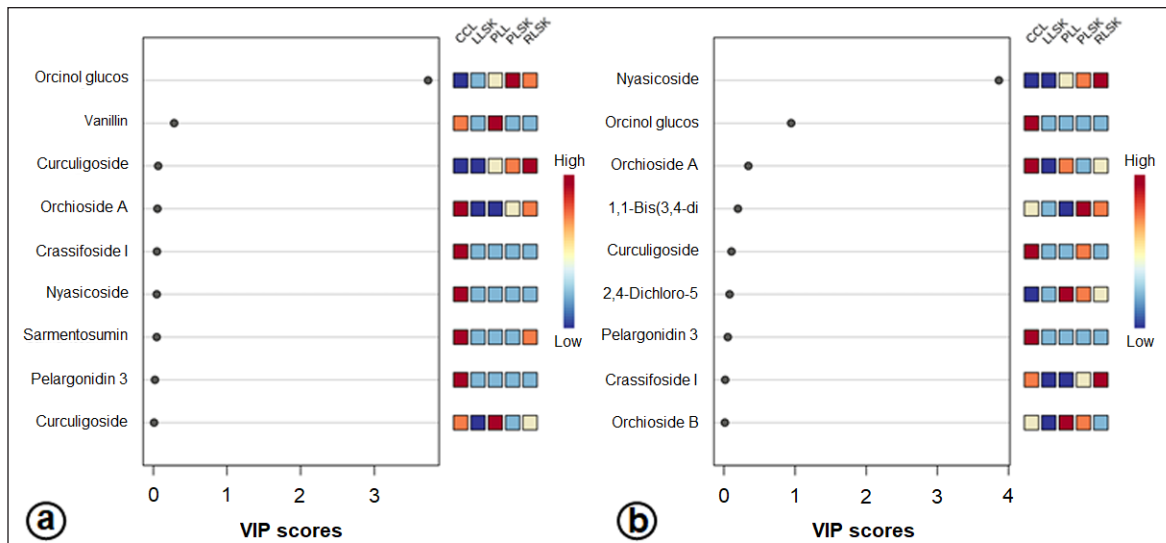


Figure 4. Importance in projection (VIP) scores of bioactive metabolites in PLS-DA at positive (a) and negative (b) modes. *In vitro* propagules and mother plant organs represented the peak area. The colored boxes (on the right) indicate the relative concentration of the corresponding metabolites. The red color indicates a high level, and the blue indicates a low level.

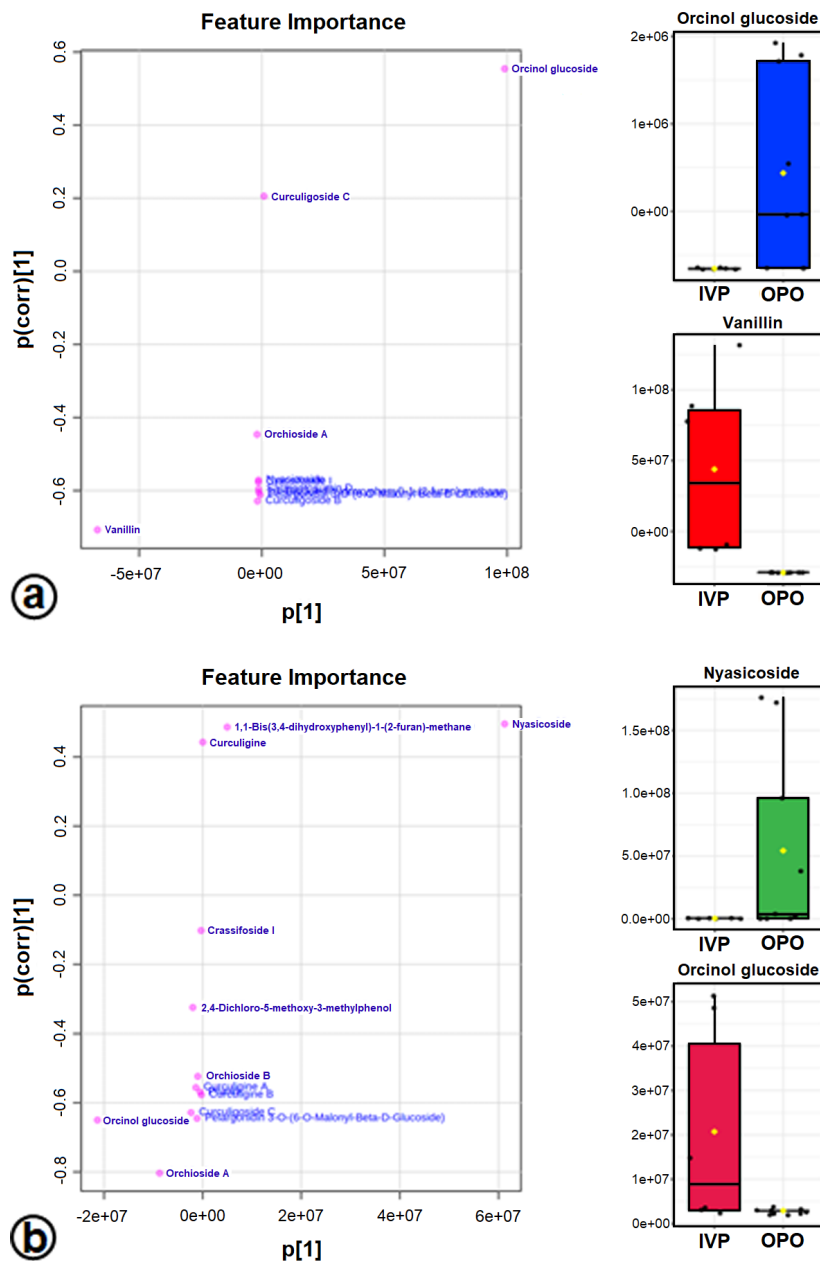


Figure 5. The OPLS-DA loadings S-plot and the compounds distinguishing the IVP from the OPO in positive (a) and negative (b) modes. Orcinol glucoside, vanillin, and nyasicoside are the marker compounds in *in vitro* propagules and in mother plant organs.

DISCUSSION

Phenolic compounds have widely attracted attention due to their potential as antioxidants and their ability to reduce the generation and scavenge free radicals. In this study, the highest phenolic content was found in the rhizome (Table 1). This high level of total phenolics is supported by the results of the metabolite profiling that we have carried out (Table 2). The high level of phenolics is most probably influenced by the soil pH and micronutrient content. In the rainy season, the increase of micronutrient solubility results in the decrease of the soil pH, which can be attributed to lower mineralization processes at lower

pH. Micronutrients in the soil directly affect the biosynthesis and concentration of secondary metabolites in plants, augmenting the phenolics content (Kumar *et al.*, 2022). The accumulation of secondary metabolites was reported to have an essential role in plant tolerance to biotic and abiotic stresses. The plants adapt to fluctuating environmental conditions, among others, due to their high phenolic content and their antioxidant capacity (Hashim *et al.*, 2020). Callus and plantlet leave also accumulated a relatively high level of phenols. It is generally accepted that phenolic compounds act synergistically with auxin in the developing callus and organs. A high level of phenolics protects auxin from

oxidation, making it more effective (Jagiello-Kubiec *et al.*, 2021). The environmental condition and plant growth stage influence the secondary metabolite content and composition (Yeshi *et al.*, 2022).

The antioxidant activity of plant extracts cannot be evaluated by a single method because of the complex nature of phytochemicals, and the determination of antioxidant activity is highly dependent on the reaction mechanism (Yaermaimaiti *et al.*, 2021). Several chemical or biological assays have been developed to evaluate their antioxidant activity and explain the action mechanism of an antioxidant in plant extracts. The DPPH, ABTS, and reducing power tests are the most commonly used (Lee and Cho, 2021; Yaermaimaiti *et al.*, 2021). Therefore, in this study, we also employed different methods to compare the antioxidant potential of *in vitro* propagules and the field-raised mother plant organs of *C. latifolia*. Many antioxidants react with DPPH by the hydrogen-atom transfer mechanism or the single electron transfer mechanism (SET), depending on the antioxidants, free radicals, and the reaction environment. ABTS has the exact mechanism of action as the DPPH, as these two radicals (DPPH and ABTS) are soluble in water and in organic solvents, but SET seems to be the primary mechanism occurring in the DPPH assay (Baschieri and Amorati, 2021). IC_{50} is a parameter widely used in measuring antioxidant activity, including DPPH and ABTS. A lower IC_{50} value indicates higher antioxidant activity (Trinh *et al.*, 2022). The FRAP assay helps in establishing the reductive activity by reducing Fe (III) to Fe (II) under acidic conditions, presenting the ability of the compound to reduce free radicals via electron transfer (Butkeviciute *et al.*, 2021). Differences in the antioxidant activity values are due to the different mechanisms of each method taken to measure antioxidant activities (Xu *et al.*, 2019). In this study, the rhizome extract exhibited the best antioxidant activity (DPPH and ABTS), probably due to the high level of total phenolics, while with the FRAP method, the highest antioxidant activity was obtained from the leaf extract, although its phenolic content was moderate. This fact drove us to assume that phenolics do not exert this property in leaves. It might probably be undertaken by norlignan, sitosterol, or cycloartane, also identified in this organ (Table S1). As reported by Li *et al.* (2012) by the DPPH method, norlignan of *in vitro* *Curculigo sinensis* showed strong radical scavenging activities. By the DPPH, ABTS, and FRAP methods, sitosterol from *Phlomis thapsoides* had antioxidant ability (Sobeh *et al.*, 2016), and cycloartane of *Astragalus plumosus* demonstrated the potential for antioxidant activity (Denizli *et al.*, 2014).

The antioxidant capacities from the DPPH, ABTS, and FRAP methods on the *in vitro* propagules and organs of *C. latifolia* gave different results. Callus and plantlet leaves had better antioxidant activity than the leaves and petiole of the mother plant. By DPPH and superoxide dismutase assays, Farzinebrahimi *et al.* (2016) also reported that the callus of this species has potential components as an antioxidant. Additionally, they noticed that callus generated from rhizomal explant and rhizome collected from the field performed superior antioxidant activities than those from leaf-derived callus and the original leaves. A similar result was also obtained by Hejazi *et al.* (2018) and Kushalan *et al.* (2022), who reported that the rhizome of *Curculigo orchiooides* had the highest activity as an antioxidant. Based on the collected information and our results, it is suggested that the rhizome of *Curculigo* spp. is the main site of secondary metabolites accumulation, at least those exerting as antioxidants. In this study, the leaves and plantlet leaves of *C. latifolia* have lower antioxidant activity than the rhizomes. Our previous study

(Umar *et al.*, 2021a) revealed that the leaves of *C. latifolia* and *C. orchiooides* had a high level of total flavonoids compared to other organs. Flavonoids that are also included in the phenolic group have synergistic or opposite effects as antioxidants.

UHPLC-Q-Orbitrap HRMS has been widely used to characterize metabolites in a complex mixture, particularly in *in vitro* propagules (López-Ramírez *et al.*, 2021; Ramabulana *et al.*, 2021). We identified 27 tentative compounds in the callus and plantlet leaves (Table S1). In general, the compounds were dominated by phenolics, and the other significant groups were alkaloids, steroids, and terpenoids. A study by Umar *et al.* (2021a) found that the compounds having antioxidant and α -glucosidase inhibition effects in *C. latifolia* were 1,1-bis-(3,4-dihydroxyphenyl)-1-(2-furan)-methane, (1S,2R)-*O*-methylmyricoside, 2,4-dichloro-5-methoxy-3-methylphenol, curculigoside B, curculigosaponin G, H, and I, orchioside B, and orcinol glucoside. They were identified in the mother plant organs as well as in the callus and plantlet leaves. Similar compound types in plant organs and *in vitro* propagules might originate from similar biosynthetic pathways.

Figure 2 shows that several compounds identified in plantlet leaves had higher concentrations (peak area) than those in the callus and mother plant organs. The plantlets were cultured on MS basal medium with plant growth regulators. Plant callus as an alternative source of raw material can be induced to increase its metabolites content through several interventions, for example, by adding biotic or abiotic elicitors (Ferdausi *et al.*, 2021), manipulating biosynthetic pathways (Inyai *et al.*, 2021), or genetic engineering (Shi *et al.*, 2021).

Differences were detected in the chromatogram pattern and tentative analysis of compounds in the callus, plantlet leaves, and plant organs. Concentration differences in various *in vitro* propagules had been reported in *Bidens pilosa* (Ramabulana *et al.*, 2021), *Cleome dendroides* (de Castro *et al.*, 2021), and *Nelumbo nucifera* (Deng *et al.*, 2020). The gap in quinine concentration between *Cinchona ledgeriana in vitro* cells and plant organs (Ratnadewi *et al.*, 2021) and variable substance composition in *in vitro* propagules and mother plant organs of *Saraca asoca* (Vignesh *et al.*, 2022) have been stated. Those differences may be due to the absence of intercellular translocation in the cultured cells (Ratnadewi *et al.*, 2021), the types of plant growth regulators used versus the natural hormones (Babich *et al.*, 2021), and the employment of elicitors (Rady *et al.*, 2021).

Untargeted metabolomic analysis is a comprehensive assessment to get an overall picture of metabolites and to systematically identify and quantify any essential metabolites from a biological sample (Zhang *et al.*, 2011). Compounds found in several other plant species were also identified in the CCL, including pelargonidin 3-*O*-(6-*O*-malonyl-beta-*D*-glucoside), which belongs to anthocyanin of *Kadsura coccinea* (Huang *et al.*, 2021); sarmentosumin D in *Piper sarmentosum*, used to treat vascular endothelial dysfunction (Md. Salleh *et al.*, 2021); ecdysterone, a steroid found in *Achyranthes bidentata*, used to treat various degenerative diseases (Dinan *et al.*, 2021); salidroside in *Rhodiola rosea*, used as a neuroprotective (Zhu *et al.*, 2021). In *C. latifolia* plantlet leaves, we found some prunins, while prunin from *Prunus persica* was used as an antiobesity agent (Li *et al.*, 2021). In the oriental regions where herbal medication is commonly practiced, like in Indonesia, research on the composition and quantity of any suspected bioactive is encouraged to support local hereditary wisdom.

Due to the extensive information and data complexity, approaches with unsupervised methods, such as PCA and HCA, were used to identify the differences among samples (Ramabulana *et al.*, 2021). PCA, with principal components 1 (PC1) and 2 (PC2), collectively accounted for 100% and 99.1% at the total variance's positive and negative modes. This value showed excellent accuracy and differentiation among the samples (Lella *et al.*, 2021), in this case among the callus, plantlet leaves, and the original organs (rhizome, petiole, and leaves). In this study, the HCA supports the clustering of the sample in the PCA.

A supervised PLS-DA evaluated differences in metabolite levels in *in vitro* propagules and mother plant organs. The important variables in interpreting the PLS-DA data are VIP. The basis for ranking the metabolites was their VIP scores; only top-ranking metabolites with the highest VIP scores were considered (Wang *et al.*, 2021). Metabolites with VIP values > 1 are suspected of playing an essential role in differentiating the sample (Mashiane *et al.*, 2021). The OPLS-DA model was used to determine the marker compounds among the samples studied (Mashiane *et al.*, 2021). The marker compounds, orcinol glucoside, nyasicoside, and vanillin, were detected in this study; they have been reported to have an antioxidant capacity (Bai *et al.*, 2021; Hoque *et al.*, 2021; Wang *et al.*, 2021). These compounds could be developed as a reliable chemical marker to distinguish the *in vitro* propagules from the mother plant organs of *C. latifolia*. Complex chemical components in plants are very difficult to evaluate; thereby, specificity is needed using one or several chemical markers (chemical reference substance). In addition, chemical markers are also used for quality control of traditional medicinal raw materials (Wang *et al.*, 2022).

CONCLUSION

Phenolic groups generally dominated the secondary metabolites in *C. latifolia*. Rhizome had the highest TPC and antioxidant activity (DPPH and ABTS), followed by the plantlet leaves and callus. However, FRAP analysis indicated that there were substances other than phenolics that function as antioxidants too. *In vitro* propagules have great potential as sources of antioxidants. This information would be valuable for herbalists or herbal medicine producers in using the plant organs as well as the *in vitro* callus. Orcinol glucoside, nyasicoside, and vanillin are reliable marker compounds in discriminating the *in vitro* propagules and the mother plant organs of *C. latifolia*.

AUTHOR CONTRIBUTIONS

Abdul Halim Umar, Diah Ratnadewi, and Mohamad Rafi: Conceptualization, Methodology; Abdul Halim Umar: Collect plant samples; Abdul Halim Umar, Diah Ratnadewi, and Mohamad Rafi: Software, Validation, Data curation, Formal analysis; Abdul Halim Umar: Writing-original draft preparation; Abdul Halim Umar, Diah Ratnadewi, Mohamad Rafi, Yohana Caecilia Sulistyarningsih, and Hamim Hamim: Writing-Reviewing and Editing. All authors have read and agreed to the published manuscript.

FINANCIAL SUPPORT

The authors gratefully acknowledged the Directorate of Higher Education, the Ministry of Research and Higher Education the Republic of Indonesia for funding this research, which is part of the scholarship (BPP-DN Scheme 2017–2020) granted to Abdul Halim Umar.

CONFLICT OF INTEREST

No potential conflicts of interest were reported by the authors.

ETHICAL APPROVALS

This study does not involve experiments on animals or human subjects.

DATA AVAILABILITY

The authors confirm that the data supporting the findings of this study are available within the article and its supplementary materials.

PUBLISHER'S NOTE

This journal remains neutral with regard to jurisdictional claims in published institutional affiliation.

REFERENCES

- Babich O, Sukhikh S, Pungin A, Astahova L, Chupakhin E, Belova D, Prosekov A, Ivanova S. Evaluation of the conditions for the cultivation of callus cultures of *Hyssopus officinalis* regarding the yield of polyphenolic compounds. *Plants*, 2021; 10:915.
- Bai Y, Jian J, Liu D, Zhao X. Synthesis, characterization and application of a new biomass-based antioxidant derived from vanillin and methyl ethyl ketone. *J Clean Prod*, 2021; 316:128315.
- Baschieri A, Amorati R. Methods to determine chain-breaking antioxidant activity of nanomaterials beyond DPPH: a review. *Antioxidants*, 2021; 10:1551.
- Bertol G, Cobre AF, Pontarolo R. Differentiation of *Mikania glomerata* and *Mikania laevigata* species through mid-infrared spectroscopy and chemometrics guided by HPLC-DAD analyses. *Rev Bras Farmacogn*, 2021; 31:442–52.
- Butkeviciute A, Petrikaite V, Jurgaityte V, Liaudanskas M, Janulis V. Antioxidant, anti-inflammatory, and cytotoxic activity of extracts from some commercial apple cultivars in two colorectal and glioblastoma human cell lines. *Antioxidants*, 2021; 10:1098.
- Cabañas-García E, Areche C, Gómez-Aguirre YA, Borquez J, Muñoz R, Cruz-Sosa F, Balch EPM. Biomass production and secondary metabolite identification in callus cultures of *Coryphantha macromeris* (Engelm.) Britton & Rose (Cactaceae), a traditional medicinal plant. *S Afr J Bot*, 2021; 137:1–9; doi:10.1016/j.sajb.2020.10.002
- Chong J, Wishart DS, Xia J. Using MetaboAnalyst 4.0 for comprehensive and integrative metabolomics data analysis. *Curr Protoc Bioinformatics*, 2019; 68:e86.
- de Castro TC, Simões-Gurgel C, Gayer CR, Coelho MGP, Albarello N. Micropropagation of *Cleome dendroides* (Cleomaceae), an endemic Brazilian species, as a source of glucosinolates. *Plant Biosyst*, 2021; 155:281–90.
- Deng X, Xiong Y, Li J, Yang D, Liu J, Sun H, Song H, Wang Y, Ma J, Liu Y, Yang M. The establishment of an efficient callus induction system for lotus (*Nelumbo nucifera*). *Plants*, 2020; 9:1436.
- Denizli N, Horo I, Gülcemal D, Masullo M, Festa M, Capasso A, Koz Ö, Piacente S, Alankuş-Çalışkan Ö. Cycloartane glycosides from *Astragalus plumosus* var. *krugianus* and evaluation of their antioxidant potential. *Fitoterapia*, 2014; 92:211–8.
- Dinan L, Dioh W, Veillet S, Lafont R. 20-Hydroxyecdysone, from plant extracts to clinical use: therapeutic potential for the treatment of neuromuscular, cardio-metabolic and respiratory diseases. *Biomedicines*, 2021; 9:492.
- Farzinebrahimi R, Mat Taha R, Rashid KA, Ali Ahmed B, Danaee M, Rozali SE. Preliminary screening of antioxidant and antibacterial activities and establishment of an efficient callus induction in *Curculigo latifolia* Dryand (Lemba). *Evid Based Complement Alternat Med*, 2016; 2016:e6429652.

- Ferdausi A, Chang X, Jones M. Enhancement of galanthamine production through elicitation and NMR-based metabolite profiling in *Narcissus pseudonarcissus* cv. Carlton in vitro callus cultures. *In Vitro Cell Dev Biol-Plant*, 2021; 57:435–46.
- Han J, Wan M, Ma Z, Hu C, Yi H. Prediction of targets of Curculigoside A in osteoporosis and rheumatoid arthritis using network pharmacology and experimental verification. *Drug Des Devel Ther*, 2020; 14:5235–50.
- Hashim AM, Alharbi BM, Abdulmajeed AM, Elkelish A, Hozzein WN, Hassan HM. Oxidative stress responses of some endemic plants to high altitudes by intensifying antioxidants and secondary metabolites content. *Plants*, 2020; 9:869.
- Hejazi II, Khanam R, Mehdi SH, Bhat AR, Rizvi MMA, Thakur SC, Athar F. Antioxidative and anti-proliferative potential of *Curculigo orchoides* Gaertn in oxidative stress induced cytotoxicity: in vivo, ex vivo and in silico studies. *Food Chem Toxicol*, 2018; 115:244–59.
- Hoque MdA, Ahmad S, Chakrabarty N, Khan MF, Hafez Kabir MS, Brishti A, Raihan MdO, Alam AHMK, Haque Md. Anwarul, Nasrin MstS, Haque Md. Areeful, Reza ASMA. Antioxidative role of palm grass rhizome ameliorates anxiety and depression in experimental rodents and computer-aided model. *Heliyo*, 2021; 7:e08199.
- Huang D, Ming R, Yao S, Li L, Huang R, Tan Y. Identification of anthocyanins in the fruits of *Kadsura coccinea* using UPLC-MS/MS-based metabolomics. *Biochem Syst Ecol*, 2021; 98:104324.
- Inyai C, Yusakul G, Komaikul J, Kitisripanya T, Likhithwitayawuid K, Sritularak B, Putalun W. Improvement of stilbene production by mulberry *Morus alba* root culture via precursor feeding and co-elicitation. *Bioprocess Biosyst Eng*, 2021; 44:653–60.
- Jagiello-Kubiec K, Nowakowska K, Łukaszewska AJ, Pacholczak A. Morpho-anatomical and biochemical changes associated with rooting of micropropagated ninebark cuttings. *Plant Cell Tiss Organ Cult*, 2021; 147:229–37.
- Kim WS, Seo JH, Lee JI, Ko ES, Cho SM, Kang JR, Jeong JH, Jeong YJ, Kim CY, Cha JD, Ryu YB. The metabolite profile in culture supernatant of *Aster yomena* callus and its anti-photoaging effect in skin cells exposed to UVB. *Plants*, 2021; 10:659.
- Kumar D, Punetha A, Verma PPS, Padalia RC. Micronutrient based approach to increase yield and quality of essential oil in aromatic crops. *J Appl Res Med Aromat Plants*, 2022; 26:100361.
- Kushalan S, Yathisha UG, Khyahrii SA, Hegde S. Phytochemical and anti-oxidant evaluation of in vitro and in vivo propagated plants of *Curculigo orchoides*. *In Vitro Cell Dev Biol-Plant*, 2022; 58:382–91.
- Lee JH, Cho YS. Assessment of phenolic profiles from various organs in different species of perilla plant (*Perilla frutescens* (L.) Britt.) and their antioxidant and enzyme inhibitory potential. *Ind Crops Prod*, 2021; 171:113914.
- Lella SD, Porta NL, Tognetti R, Lombardi F, Nardin T, Larcher R. White rot fungal impact on the evolution of simple phenols during decay of silver fir wood by UHPLC-HQOMS. *Phytochem Anal*, 2021; 33:170–83.
- Li L, Li S, Cui Z, Wang Y, Li Y, Kong L, Luo J. Improving sesquiterpenoids production of *Sarcandra glabra* callus culture. *Ind Crops Prod*, 2021; 169:113636.
- Li N, Li SP, Wang KJ, Yan GQ, Zhu YY. Novel norlignan glucosides from rhizomes of *Curculigo sinensis*. *Carbohydr Res*, 2012; 351:64–67.
- López-Ramírez Y, Cabañas-García E, Areche C, Trejo-Tapia G, Pérez-Molphe-Balch E, Gómez-Aguirre YA. Callus induction and phytochemical profiling of *Yucca carnerosana* (Trel.) McKelvey obtained from in vitro cultures. *Rev Mex Ing Quim*, 2021; 20:823–37.
- Mashiane P, Manhivi VE, Shoko T, Slabbert RM, Sultanbawa Y, Sivakumar D. Cooking african pumpkin leaves (*Momordica balsamina* L.) by stir-frying improved bioactivity and bioaccessibility of metabolites-metabolomic and chemometric approaches. *Foods*, 2021; 10:2890.
- Md. Salleh MFRR, Aminuddin A, Hamid AA, Salamt N, Japar Sidik FZ, Ugusman A. *Piper sarmentosum* Roxb. attenuates vascular endothelial dysfunction in nicotine-induced rats. *Front Pharmacol*, 2021; 12:667102.
- Murashige T, Skoog F. A revised medium for rapid growth and bio assays with tobacco tissue cultures. *Physiol Plant*, 1962; 15:473–97.
- Okubo S, Terauchi K, Okada S, Saito Y, Yamaura T, Misaka T, Nakajima K, Abe K, Asakura T. De novo transcriptome analysis and comparative expression profiling of genes associated with the taste-modifying protein neoculin in *Curculigo latifolia* and *Curculigo capitulata* fruits. *BMC Genom*, 2021; 22:347.
- R Core Team. R: a language and environment for statistical computing. R Foundation for Statistical Computing, Vienna, Austria, 2018.
- Rady MR, Gierczik K, Ibrahim MM, Matter MA, Galiba G. Anticancer compounds production in *Catharanthus roseus* by methyl jasmonate and UV-B elicitation. *S Afr J Bot*, 2021; 142:34–41.
- Ramabulana AT, Steenkamp PA, Madala NE, Dubery IA. Application of plant growth regulators modulates the profile of chlorogenic acids in cultured *Bidens pilosa* cells. *Plants*, 2021; 10:437.
- Ratnadewi D, Fendiyanto MH, Satrio RD, Miftahudin M, Laili AN. Strictosidine synthase coding gene expression towards quinine biosynthesis and accumulation: inconsistency in cultured cells and fresh tissues of *Cinchona ledgeriana*. *Int J Agric Biol*, 2021; 26:131–8.
- Shi M, Liao P, Nile SH, Georgiev MI, Kai G. Biotechnological exploration of transformed root culture for value-added products. *Trends Biotechnol*, 2021; 39:137–49.
- Silalahi M, Nisyawati N. The ethnobotanical study of edible and medicinal plants in the home garden of Batak Karo sub-ethnic in North Sumatra, Indonesia. *Biodiversitas*, 2018; 19:229–38.
- Sobeh M, Mamadaliyeva NZ, Mohamed T, Krstin S, Youssef FS, Ashour ML, Azimova SS, Wink M. Chemical profiling of *Phlomis thapsoides* (Lamiaceae) and in vitro testing of its biological activities. *Med Chem Res*, 2016; 25:2304–15.
- Trinh NTN, Tuan NN, Thang TD, Kuo PC, Thanh NB, Tam LN, Tuoi LH, Nguyen THD, Vu DC, Ho TL, Anh LN, Thuy NTT. Chemical composition analysis and antioxidant activity of *Coffea robusta* monofloral honeys from Vietnam. *Foods*, 2022; 11:388.
- Tsugawa H, Cajka T, Kind T, Ma Y, Higgins B, Ikeda K, Kanazawa M, Vander Gheynst J, Fiehn O, Arita M. MS-DIAL: data-independent MS/MS deconvolution for comprehensive metabolome analysis. *Nat Methods*, 2015; 12:523–6.
- Umar AH, Ratnadewi D, Rafi M, Sulistyanyingsih YC. Untargeted metabolomics analysis using FTIR and UHPLC-Q-Orbitrap HRMS of two *Curculigo* species and evaluation of their antioxidant and α -glucosidase inhibitory activities. *Metabolites*, 2021a; 11:42.
- Umar AH, Ratnadewi D, Rafi M, Sulistyanyingsih YC, Hamim H. Callus of *Curculigo latifolia* Dryand. ex W.T.Aiton: initiation, regeneration, secretory structure and histochemistry. *IOP Conf Ser Earth Environ Sci*, 2021b; 948:012051.
- Vignesh A, Selvakumar S, Vasanth K. Comparative LC-MS analysis of bioactive compounds, antioxidants and antibacterial activity from leaf and callus extracts of *Saraca asoca*. *Phytomed Plus*, 2022; 2:100167.
- Wang R, Qin Y, Zhou J, Wang J, Shu H, Zhou S, Peng X. Comprehensive evaluation of *Bletilla striata* and its substitutes by combining phenotypic characteristic, chemical composition, and anti-melanogenic activity. *Phytochemistry*, 2022; 195:113059.
- Wang Y, Li J, Li N. Phytochemistry and pharmacological activity of plants of genus *Curculigo*: an updated review since 2013. *Molecules*, 2021; 26:3396.
- Xu YB, Chen GL, Guo MQ. Antioxidant and anti-inflammatory activities of the crude extracts of *Moringa oleifera* from Kenya and their correlations with flavonoids. *Antioxidants*, 2019; 8:296.
- Yaermaimaiti S, Wu T, Aisa HA. Bioassay-guided isolation of antioxidant, antimicrobial, and antiviral constituents of *Cordia dichotoma* fruits. *Ind Crops Prod*, 2021; 172:113977.
- Yeshi K, Crayn D, Ritmejerjetye E, Wangchuk P. Plant secondary metabolites produced in response to abiotic stresses has potential application in pharmaceutical product development. *Molecules*, 2022; 27:313.

Zhang A, Sun H, Wang P, Han Y, Wang X. Modern analytical techniques in metabolomics analysis. *Analyst*, 2011; 137:293–300.

Zhang Y, Ge JF, Wang FF, Liu F, Shi C, Li N. Crassifoside H improve the depressive-like behavior of rats under chronic unpredictable mild stress: possible involved mechanisms. *Brain Res Bull*, 2017; 135:77–84.

Zhao Y, Guo Y, Chen Y, Liu S, Wu N, Jia D. Curculigoside attenuates myocardial ischemia-reperfusion injury by inhibiting the opening of the mitochondrial permeability transition pore. *Int J Mol Med*, 2020; 45:1514–24.

Zhu L, Liu Z, Ren Y, Wu X, Liu Y, Wang T, Li Y, Cong Y, Guo Y. Neuroprotective effects of salidroside on ageing hippocampal neurons and naturally ageing mice via the PI3K/Akt/TERT pathway. *Phytother Res*, 2021; 35:5767–80.

Zhu FB, Wang JY, Zhang YL, Quan RF, Yue ZS, Zeng LR, Zheng WJ, Hou Q, Yan SG, Hu YG. Curculigoside regulates proliferation, differentiation, and pro-inflammatory cytokines levels in dexamethasone-induced rat calvarial osteoblasts. *Int J Clin Exp Med*, 2015a; 8:12337–46.

Zhu MZ, Wu W, Jiao LL, Yang PF, Guo MQ. Analysis of flavonoids in lotus (*Nelumbo nucifera*) leaves and their antioxidant activity using macroporous resin chromatography coupled with LC-MS/MS and antioxidant biochemical assays. *Molecules*, 2015b; 20:10553–65.

How to cite this article:

Umar AH, Ratnadewi D, Rafi M, Sulistyarningsih YC, Hamim H. Phenolics profile and antioxidant activities of *in vitro* propagules and field-raised plant organs of *Curculigo latifolia*. *J Appl Pharm Sci*, 2023; 13(04):168–185.

SUPPLEMENTARY MATERIAL

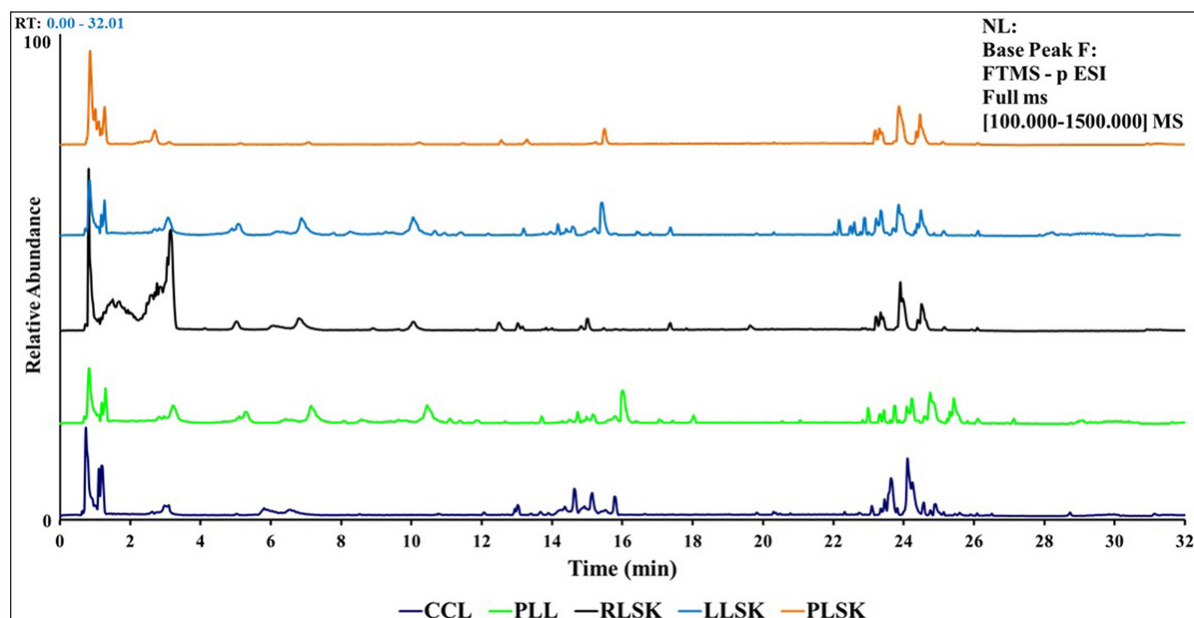


Figure S1. UHPLC-Q-Orbitrap HRMS chromatogram of 70% ethanol extract from CCL, PLL, RLSK, LLSK, and PLSK of *C. latifolia*.

Table S1. Compounds identified in 70% ethanol extract from CCL, PLL, RLSK, LLSK, and PLSK of *C. latifolia*.

CCL									
No.	RT[min]	Adduct ion	Formula	Tentative identification	Expected <i>m/z</i>	Experimental <i>m/z</i>	Accuracy (ppm)	Fragment MS and MS/MS	Chemical type
1	0.87	[M – H] ⁻	C ₂₃ H ₂₆ O ₁₀	Orchioside B	461.153	461.157	-8.674	443.134; 433.150; 371.113	Phenolic glycosides
2	0.90	[M – H] ⁻	C ₁₇ H ₁₄ O ₅	1,1-bis(3,4-dihydroxyphenyl)-1-(2-furan)-methane	297.084	297.082	6.732	281.045; 269.081	Phenolic
3	1.33	[M + H] ⁺	C ₈ H ₈ O ₃	Vanillin	153.047	153.047	0.000	150.981; 137.018; 136.015; 129.113	Phenolic
4	2.33	[M + H] ⁺	C ₂₃ H ₂₄ O ₁₁	Crassifoside I	477.132	477.137	-10.479	457.114; 445.114; 387.108	Phenolic
5	3.29	[M – H] ⁻	C ₁₃ H ₁₈ O ₇	Orcinol glucoside	285.105	285.105	0.000	285.105	Phenolic glycosides
6	7.49	[M + H] ⁺	C ₂₃ H ₂₆ O ₁₁	Nyasicoside	479.148	479.152	-8.348	479.152	Phenolic
7	13.62	[M – H] ⁻	C ₂₄ H ₂₃ O ₁₃	Pelargonidin 3- <i>O</i> -(6- <i>O</i> -malonyl-beta- <i>D</i> -glucoside)	518.114	518.116	-3.860	285.170; 257.175; 243.159	Flavonoid
8	14.02	[M + H] ⁺	C ₂₄ H ₂₃ O ₁₃	Pelargonidin 3- <i>O</i> -(6- <i>O</i> -malonyl-beta- <i>D</i> -glucoside)	520.114	520.114	0.000	433.113; 271.061	Flavonoid
9	14.57	[M – H] ⁻	C ₂₂ H ₂₆ O ₁₁	Orchioside A	465.148	465.149	-2.150	449.108; 447.129; 435.129	Phenolic glycosides
10	14.81	[M + H] ⁺	C ₂₁ H ₂₄ O ₁₁	Curculigoside B	453.132	453.130	4.414	290.271; 276.244	Phenolic glycosides
11	15.07	[M + H] ⁺	C ₂₂ H ₂₆ O ₁₁	Orchioside A	467.148	467.148	0.000	350.143; 213.143	Phenolic glycosides
12	15.44	[M + H] ⁺	C ₅₀ H ₄₂ O ₉	Sarmentosumin D	787.283	787.281	2.540	769.279; 759.295; 691.232	Flavanone

Continued

No.	RT[min]	Adduct ion	Formula	Tentative identification	Expected <i>m/z</i>	Experimental <i>m/z</i>	Accuracy (ppm)	Fragment MS and MS/MS	Chemical type
13	15.97	[M – H] ⁻	C ₂₃ H ₂₄ O ₁₁	Crassifoside I	475.132	475.129	6.314	457.114; 445.114; 387.108	Phenolic
14	16.31	[M + H] ⁺	C ₂₇ H ₄₄ O ₇	Ecdysterone	481.309	481.304	10.388	473.333; 467.106; 454.833; 451.750	Sterol
15	17.59	[M – H] ⁻	C ₂₂ H ₂₆ O ₁₂	Curculigoside C	481.142	481.140	4.157	463.124; 453.140; 451.124	Phenolic glycosides
16	17.91	[M + H] ⁺	C ₂₈ H ₂₂ O ₁₁	Theanaphthoquinone	535.116	535.116	0.000	517.112; 507.128; 477.118	Quinones
17	19.61	[M – H] ⁻	C ₃₂ H ₄₀ O ₇	Longirostrerone A	535.277	535.276	1.868	535.277	Azaphilones
18	19.75	[M + H] ⁺	C ₂₆ H ₃₈ O ₁₆	Pothobanoside C	607.216	607.214	3.294	607.214	Hemiterpene glucoside
19	20.09	[M – H] ⁻	C ₁₄ H ₂₀ O ₇	Salidroside	299.121	299.123	-6.686	299.123	Glucoside
20	21.65	[M – H] ⁻	C ₂₂ H ₂₄ O ₁₀	Neosakuranin	447.137	447.135	4.473	447.135	Chalcone glycoside
21	21.98	[M – H] ⁻	C ₂₁ H ₁₈ O ₁₂	Breviscapin	461.080	461.081	-2.169	285.040; 267.029; 257.045; 243.029	Glucuronates
22	22.10	[M – H] ⁻	C ₂₃ H ₂₆ O ₁₁	Nyasicoside	477.148	477.144	8.383	459.129; 449.145; 447.129	Phenolic
23	22.41	[M + H] ⁺	C ₃₂ H ₄₀ O ₇	Longirostrerone A	537.277	537.275	3.722	537.275	Azaphilones
24	25.67	[M + H] ⁺	C ₂₇ H ₃₈ O ₁₄	Laciniatoside V	587.226	587.223	5.109	569.222; 407.170; 393.154; 343.175	Iridoid glucoside
25	26.04	[M – H] ⁻	C ₃₀ H ₂₀ O ₈	Emodin Dianthrone	507.116	507.116	0.000	491.077; 467.077; 441.097; 425.066	Glycosides
26	27.27	[M + H] ⁺	C ₃₆ H ₇₀ O ₂	3-methoxy-5-acetyl-31-tritriacontene	535.538	535.537	1.867	535.537	-
27	30.92	[M + H] ⁺	C ₄₁ H ₆₈ O ₁₃	Curculigosaponin C	769.466	769.466	0.000	606.413; 474.370	Cycloartane triterpene

PLL

No.	RT[min]	Adduction	Formula	Tentative identification	Expected <i>m/z</i>	Experimental <i>m/z</i>	Accuracy (ppm)	Fragment MS and MS/MS	Chemical type
1	0.92	[M + H] ⁺	C ₁₇ H ₁₄ O ₅	1,1-bis(3,4-dihydroxyphenyl)-1-(2-furan)-methane	299.084	299.087	-10.031	166.072	Phenolic
2	8.46	[M + H] ⁺	C ₂₁ H ₂₄ O ₁₁	Curculigoside B	453.132	453.135	-6.621	290.271; 276.244	Phenolic glycosides
3	10.08	[M + H] ⁺	C ₈ H ₈ O ₃	Vanillin	153.047	153.047	0.000	150.981; 137.018; 136.015; 129.113	Phenolic
4	12.35	[M + H] ⁺	C ₁₅ H ₂₆ O ₃	Capitulatin B	255.188	255.189	-3.919	255.189	Eudesman
5	13.41	[M + H] ⁺	C ₂₄ H ₂₈ O ₁₁	(1S,2R)- <i>O</i> -methylnyasicoside	493.163	493.161	4.055	373.055	Norlignan glycosides
6	14.14	[M + H] ⁺	C ₁₆ H ₁₇ NO ₄	Lycorine	288.116	288.116	0.000	270.113; 252.102; 240.102; 216.102	Alkaloid
7	15.07	[M – H] ⁻	C ₂₂ H ₂₆ O ₁₁	Orchioside A	465.148	465.150	-4.300	449.108; 447.129; 435.129	Phenolic glycosides
8	15.30	[M + H] ⁺	C ₁₈ H ₁₈ O ₆	(1R,2R)-crassifogenin-D	331.110	331.112	-6.040	331.190; 249.112; 167.033	Norlignan glycosides
9	15.54	[M – H] ⁻	C ₂₃ H ₂₆ O ₁₀	Orchioside B	461.153	461.149	8.674	443.134; 433.150; 371.113	Phenolic glycosides

Continued

No.	RT[min]	Adduction	Formula	Tentative identification	Expected <i>m/z</i>	Experimental <i>m/z</i>	Accuracy (ppm)	Fragment MS and MS/MS	Chemical type
10	17.87	[M + H] ⁺	C ₂₂ H ₂₄ O ₁₀	Neosakuranin	449.137	449.137	0.000	449.137	Chalcone glycoside
11	19.27	[M - H] ⁻	C ₁₆ H ₁₇ NO ₄	Lycorine	286.116	286.116	0.000	270.076; 268.097; 258.076; 256.097	Alkaloid
12	19.97	[M + H] ⁺	C ₂₇ H ₄₄ O ₇	Ecdysterone	481.309	481.307	4.155	473.333; 467.106; 454.833; 451.750	Steroid
13	20.43	[M + H] ⁺	C ₂₆ H ₃₈ O ₁₆	Pothobanoside C	607.216	607.213	4.941	607.213	Hemiterpene glucoside
14	20.65	[M - H] ⁻	C ₂₀ H ₂₈ Cl ₂ O ₁₂	Curculigine A	529.096	529.099	-5.670	529.099	Phenolic glycosides
15	21.24	[M + H] ⁺	C ₁₃ H ₁₈ O ₇	Orcinol glucoside	287.105	287.105	0.000	269.100; 256.121; 254.993; 251.093; 237.020	Phenolic glycosides
16	21.70	[M + H] ⁺	C ₃₀ H ₄₈ O ₅	Asiatic acid	489.350	489.355	-10.218	453.336; 407.331; 330.222	Pentacyclic triterpene
17	22.10	[M - H] ⁻	C ₂₃ H ₂₆ O ₁₁	Nyasicoside	477.148	477.144	8.383	459.129; 449.145; 447.129	Phenolic
18	23.37	[M + H] ⁺	C ₂₂ H ₂₆ O ₁₁	Orchioside A	467.148	467.149	-2.141	350.143; 213.143	Phenolic glycosides
19	23.49	[M - H] ⁻	C ₂₁ H ₂₂ O ₁₀	Prunin	433.121	433.118	6.926	273.076; 179.034	Flavanone glycoside
20	23.99	[M - H] ⁻	C ₂₁ H ₁₈ O ₁₂	Breviscapin	461.080	461.084	-8.675	285.040; 267.029; 257.045; 243.029	Glucuronates
21	24.02	[M + H] ⁺	C ₂₂ H ₂₆ O ₁₂	Curculigoside C	483.142	483.138	8.279	465.139; 421.112	Phenolic glycosides
22	24.12	[M - H] ⁻	C ₂₁ H ₂₄ O ₁₁	Curculigoside B	451.132	451.129	6.650	433.114; 423.129	Phenolic glycosides
23	25.60	[M - H] ⁻	C ₃₀ H ₂₀ O ₈	Emodin dianthrone	507.116	507.121	-9.860	254.058	Glycosides
24	25.67	[M + H] ⁺	C ₂₇ H ₃₈ O ₁₄	Laciniatoside V	587.226	587.222	6.812	569.222; 407.170; 393.154; 343.175	Iridoid glucoside
25	27.01	[M + H] ⁺	C ₃₆ H ₇₀ O ₂	3-methoxy-5-acetyl-31-tritriacontene	535.538	535.543	-9.336	535.543	-
26	30.92	[M + H] ⁺	C ₄₁ H ₆₈ O ₁₃	Curculigosaponin C	769.466	769.466	0.000	606.413; 474.370	Cycloartane triterpene
27	31.20	[M - H] ⁻	C ₈ H ₈ Cl ₂ O ₂	2,4-dichloro-5-methoxy-3-methylphenol	204.990	204.991	-4.878	176.987; 174.972; 154.990; 150.972	Phenolic

RLSK

No.	RT [min]	Adduction	Formula	Tentative identification	Expected <i>m/z</i>	Experimental <i>m/z</i>	Accuracy (ppm)	Fragment MS and MS/MS	Chemical type
1	0.914	[M - H] ⁻	C ₁₇ H ₁₄ O ₅	1,1-bis(3,4-dihydroxyphenyl)-1-(2-furan)-methane	297.082	297.084	-6.732	281.045; 271.061; 269.081	Phenolic
2	0.930	[M + H] ⁺	C ₁₆ H ₁₇ NO ₄	Lycorine	288.116	288.116	0.000	270.113; 252.102; 240.102; 216.102	Alkaloid
3	1.334	[M + H] ⁺	C ₈ H ₈ O ₃	Vanillin	153.047	153.046	6.534	150.981; 137.018; 136.015; 129.113	Phenolic
4	1.453	[M - H] ⁻	C ₈ H ₈ Cl ₂ O ₂	2,4-dichloro-5-methoxy-3-methylphenol	204.989	204.990	-4.878	176.987; 174.972; 154.990; 150.972	Phenolic
5	2.335	[M + H] ⁺	C ₂₃ H ₂₄ O ₁₁	Crassifoside I	477.131	477.136	-10.479	457.114; 445.114; 387.108	Phenolic
6	2.783	[M + H] ⁺	C ₁₆ H ₁₇ NO ₄	Lycorine	288.115	288.116	-3.471	270.113; 252.102; 240.102; 216.102	Alkaloid
7	3.118	[M + H] ⁺	C ₁₃ H ₁₈ O ₇	Orcinol glucoside	287.107	287.105	6.966	269.100; 256.121; 254.993; 251.093; 237.020	Phenolic glycosides
8	5.832	[M - H] ⁻	C ₂₃ H ₂₈ O ₁₂	Curculigine	495.158	495.158	0.000	315.148; 161.109	Chlorophenols glucosides
9	6.376	[M + H] ⁺	C ₂₁ H ₂₄ O ₁₁	Curculigoside B	453.132	453.132	0.000	290.271; 276.244	Phenolic glycosides
10	14.135	[M + H] ⁺	C ₂₂ H ₂₆ O ₁₁	Orchioside A	467.153	467.148	10.703	305.144; 291.144	Phenolic glycosides
11	14.575	[M - H] ⁻	C ₂₂ H ₂₆ O ₁₁	Orchioside A	465.147	465.149	-4.300	449.108; 447.129; 435.129	Phenolic glycosides
12	14.021	[M + H] ⁺	C ₂₄ H ₂₃ O ₁₃	Pelargonidin 3- <i>O</i> -(6- <i>O</i> -malonyl-beta- <i>D</i> -glucoside)	520.113	520.114	-1.923	433.113; 271.061	Flavonoid
13	22.102	[M + H] ⁺	C ₂₃ H ₂₆ O ₁₁	Nyasicoside	479.147	479.151	-8.348	479.152	Phenolic
14	24.027	[M + H] ⁺	C ₂₂ H ₂₆ O ₁₂	Curculigoside C	483.142	483.137	10.349	465.139; 421.112	Phenolic glycosides
15	24.680	[M - H] ⁻	C ₂₁ H ₂₄ O ₁₁	Curculigoside B	451.128	451.132	-8.867	433.114; 423.129	Phenolic glycosides
16	24.680	[M - H] ⁻	C ₂₃ H ₂₆ O ₁₀	Orchioside B	461.157	461.153	8.674	443.134; 433.150; 371.113	Phenolic glycosides
17	30.887	[M - H] ⁻	C ₄₁ H ₆₈ O ₁₃	Curculigosaponin C	767.464	767.466	-2.606	693.421; 659.416	Cycloartane

LLSK

No.	RT [min]	Adduction	Formula	Tentative identification	Expected <i>m/z</i>	Experimental <i>m/z</i>	Accuracy (ppm)	Fragment MS and MS/MS	Chemical type
1	0.876	[M + H] ⁺	C ₁₈ H ₁₈ O ₆	(1R,2R)-crassifogenin-D	331.113	331.110	9.060	315.086; 313.107; 303.122	Norlignan
2	0.888	[M - H] ⁻	C ₁₇ H ₁₄ O ₅	1,1-bis(3,4-dihydroxyphenyl)-1-(2-furan)-methane	297.082	297.084	-6.732	281.045; 271.061; 269.081	Phenolic
3	1.332	[M + H] ⁺	C ₈ H ₈ O ₃	Vanillin	153.047	153.047	0.000	150.981; 137.018; 136.015; 129.113	Phenolic
4	7.886	[M + H] ⁺	C ₂₁ H ₂₄ O ₁₁	Curculigoside B	453.136	453.132	8.827	290.271; 276.244	Phenolic glycosides
5	14.025	[M + H] ⁺	C ₂₄ H ₂₃ O ₁₃	Pelargonidin 3- <i>O</i> -(6- <i>O</i> -malonyl-beta- <i>D</i> -glucoside)	520.113	520.113	0.000	433.113; 271.061	Flavonoid
6	14.863	[M - H] ⁻	C ₁₇ H ₁₄ O ₅	Sinensigenin B	297.084	297.084	0.000	295.173; 190.152	Norlignan
7	15.965	[M - H] ⁻	C ₂₃ H ₂₄ O ₁₁	Crassifoside I	475.131	475.129	4.209	457.114; 445.114; 387.108	Phenolic
8	24.564	[M - H] ⁻	C ₂₃ H ₂₆ O ₁₀	Orchioside B	461.157	461.153	8.674	443.134; 433.150; 371.113	Phenolic glycosides
9	20.657	[M - H] ⁻	C ₂₀ H ₂₈ Cl ₂ O ₁₂	Curculigine A	529.096	529.099	-5.670	529.099	Phenolic glycosides

Continued

No.	RT [min]	Adduction	Formula	Tentative identification	Expected <i>m/z</i>	Experimental <i>m/z</i>	Accuracy (ppm)	Fragment MS and MS/MS	Chemical type
10	24.585	[M – H] ⁻	C ₂₁ H ₂₄ O ₁₁	Curculigoside B	451.128	451.132	-8.867	433.114; 423.129	Phenolic glycosides
11	25.183	[M – H] ⁻	C ₂₂ H ₂₆ O ₁₁	Orchioside A	465.144	465.148	-8.599	449.108; 447.129; 435.129	Phenolic glycosides
12	25.658	[M – H] ⁻	C ₃₅ H ₆₀ O ₆	3- <i>O-B-D</i> -glucopyranosyl sitosterol	575.441	575.439	3.476	559.400; 547.400; 477.322	Sitosterol
13	25.931	[M – H] ⁻	C ₄₇ H ₇₈ O ₁₇	Curculigosaponin H	913.526	913.524	2.189	895.506; 883.506; 781.474; 767.458	Cycloartane
14	31.436	[M – H] ⁻	C ₈ H ₈ Cl ₂ O ₂	2,4-dichloro-5-methoxy-3-methylphenol	204.992	204.990	9.756	176.987; 174.972; 154.990; 150.972	Phenolic

PLSK

No.	RT [min]	Adduction	Formula	Tentative identification	Expected <i>m/z</i>	Experimental <i>m/z</i>	Accuracy (ppm)	Fragment MS and MS/MS	Chemical type
1	0.850	[M – H] ⁻	C ₂₃ H ₂₄ O ₁₁	Crassifoside I	475.128	475.132	-8.419	457.114; 445.114; 387.108	Phenolic
2	0.882	[M – H] ⁻	C ₁₇ H ₁₄ O ₅	1,1-bis(3,4-dihydroxyphenyl)-1-(2-furan)-methane	297.082	297.084	-6.732	281.045; 271.061; 269.081	Phenolic
3	1.442	[M – H] ⁻	C ₈ H ₈ Cl ₂ O ₂	2,4-dichloro-5-methoxy-3-methylphenol	204.990	204.990	0.000	176.987; 174.972; 154.990; 150.972	Phenolic
4	3.142	[M + H] ⁺	C ₁₆ H ₁₇ NO ₄	Lycorine	288.116	288.116	0.000	270.113; 252.102; 240.102; 216.102	Alkaloid
5	3.295	[M – H] ⁻	C ₁₃ H ₁₈ O ₇	Orcinol glucoside	285.105	285.105	0.000	285.105	Phenolic glycosides
6	3.684	[M – H] ⁻	C ₂₂ H ₂₆ O ₁₁	Orchioside A	465.150	465.148	4.300	449.108; 447.129; 435.129	Phenolic glycosides
7	6.378	[M + H] ⁺	C ₂₁ H ₂₄ O ₁₁	Curculigoside B	453.133	453.132	2.207	290.271; 276.244	Phenolic glycosides
8	19.012	[M – H] ⁻	C ₁₆ H ₁₇ NO ₄	Lycorine	286.118	286.116	6.990	270.076; 268.097; 258.076; 256.097	Alkaloid
9	23.292	[M – H] ⁻	C ₄₂ H ₇₀ O ₁₃	Curculigosaponin G	781.475	781.482	-8.957	749.448; 635.416	Cycloartane
10	24.591	[M – H] ⁻	C ₂₃ H ₂₆ O ₁₀	Orchioside B	461.157	461.153	8.674	443.134; 433.150; 371.113	Phenolic glycosides
11	24.627	[M – H] ⁻	C ₂₁ H ₂₄ O ₁₁	Curculigoside B	451.129	451.132	-6.650	433.114; 423.129	Phenolic glycosides
12	25.944	[M – H] ⁻	C ₄₇ H ₇₈ O ₁₇	Curculigosaponin H	913.524	913.524	0.000	895.506; 883.506; 781.474; 767.458	Cycloartane
13	29.206	[M – H] ⁻	C ₃₅ H ₆₀ O ₆	3- <i>O-B-D</i> -glucopyranosyl sitosterol	575.434	575.439	-8.689	559.400; 547.400; 477.322	Sitosterol
14	30.893	[M – H] ⁻	C ₄₁ H ₆₈ O ₁₃	Curculigosaponin C	767.466	767.466	0.000	693.421; 659.416	Cycloartane
15	31.027	[M – H] ⁻	C ₈ H ₈ Cl ₂ O ₂	2,4-dichloro-5-methoxy-3-methylphenol	204.992	204.990	9.756	176.987; 174.972; 154.990; 150.972	Phenolic

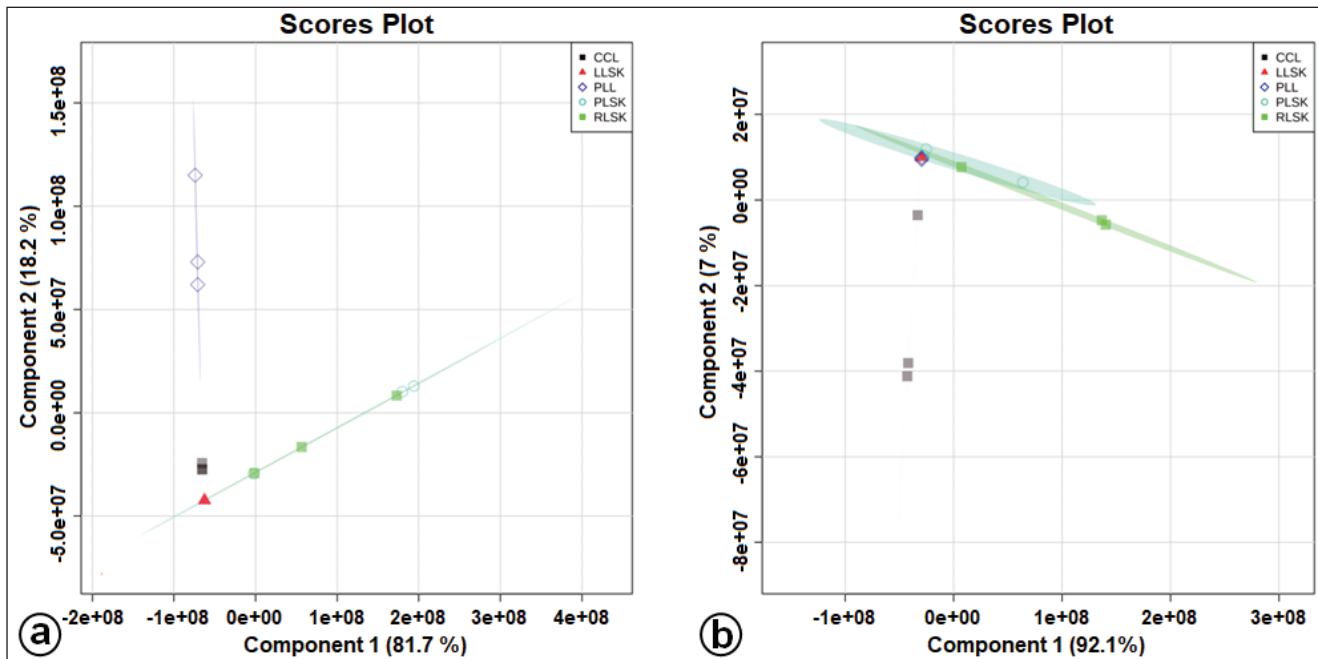


Figure S2. Supervised PLS-DA score plot showing separation of clusters for *in vitro* propagules and mother plant organs based on bioactive metabolites at positive (a) and negative (b) modes generated by the UHPLC-Q-Orbitrap HRMS analysis.

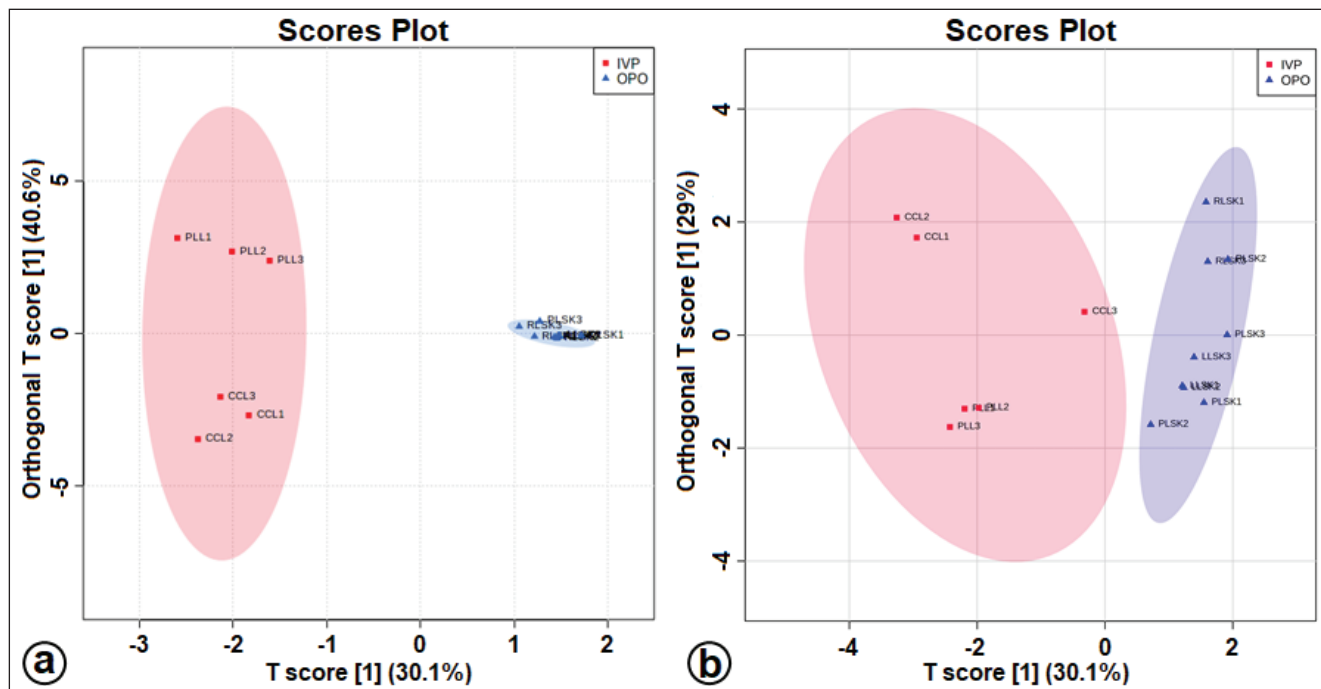


Figure S3. The OPLS-DA score plot at positive (a) and negative (b) modes for separating *in vitro* propagules and mother plant organs of *C. latifolia*.

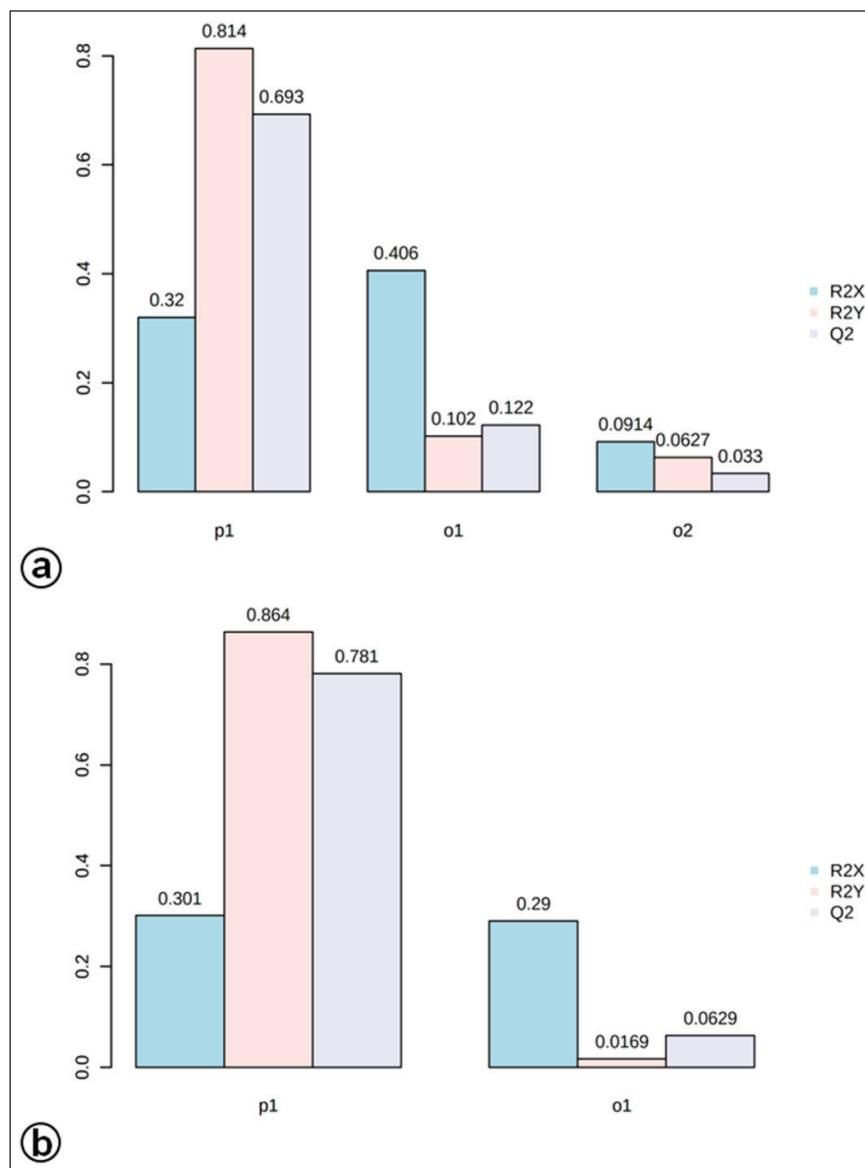


Figure S4. The OPLS-DA model shows the level of goodness-of-fit (R^2) and predictability level (Q^2) at positive (a) and negative (b) modes.